

Predictability of the Moisture Regime Associated with the Preonset of Sahelian Rainfall

Roberto J. Mera and Fredrick H.M. Semazzi

North Carolina State University

Corresponding author: rjmera@ncsu.edu

Introduction

The present study seeks to understand the predictability of the primary attributes associated with the moisture regime during the preonset period of Sahelian rainfall. The moisture regime associated with the preonset of the West African Monsoon (WAM) is of primary concern for the population in the region due to its influence in areas such as health and agriculture. The end of meningitis outbreaks, for example, tends to coincide with influx of moisture at the end the dry season (Molesworth et al. 2003). This study will serve as a compliment to work currently under development at the University Corporation for Atmospheric Research (UCAR) by evaluating the skill of the Weather Research and Forecasting Model (WRF) and other model forecasts of weather variables at spatial resolutions (district level) that are relevant to meningitis management in the region.

The preonset period of the WAM is defined as the arrival in the intertropical front (ITF) at 15°N, where the confluence line between moist southwesterly monsoon winds and dry northeasterly Harmattan occurs (Sultan and Janicot 2000; Le Barbe et al. 2002, Sultan and Janicot, 2003). This brings sufficient moisture for isolated convective systems to develop in the Sudano-Sahelian zone ahead of the Intertropical Convergence Zone (ITCZ), which during late May / early June is located at 5°N. Dynamics associated with the Saharan Heat Low (SHL) dominates the continental region in this time period. Also during this time, isolated convective systems appear over the continent, resulting in an apparent expansion of the ITCZ.

The dynamics of the monsoon winds are controlled by the pressure gradient between the heat low located over the ITF and oceanic high pressures (Santa Helena anticyclone), while the Harmattan is modulated by pressure gradients created by the SHL and the Azores and Lybian anticyclones (Sultan and Janicot, 2003). Moisture advection into West Africa throughout the dry season and the pre-onset of the monsoon can have a significant impact on the timing of the monsoon “jump” as described by Hagos and Cook (2007). It was suggested by Sultan and Janicot (2000) and Le Barbe et al. (2002) that the “jump” can be characterized as an acceleration of the seasonal cycle triggered by westward propagating convective events.

The variability of the pre-onset stage of monsoon development is one of the factors that affects the moisture regime of the region in the days and weeks prior to the onset of the WAM. Our study aims to understand the moisture conditions that precede the WAM in diurnal, interannual and intraseasonal time scales. More specifically, we focus on conditions at the surface where there is a robust, actionable relationship between meningitis mitigation and environmental conditions. Some of the more prevalent features that dictate the moisture content of the atmosphere during this time period include the intensity of rainfall along the Gulf of Guinea as described in Lebel et al (2003), the diurnal cycle of the monsoon (Parker et al., 2005), mid-latitude disturbance incursions into the region (Knippertz and Fink, 2009), transient convective systems (Flamant et al., 2007, 2009), modulation of the SHL and African Easterly Jet (AEJ) (Sultan and Janicot, 2003), and variance of orographically induced circulations (Drobinski et al., 2005).

We use the Weather Research and Forecasting (WRF) model Version 3 as a tool to diagnose the primary attributes that

dictate predictability of the moisture regime as dictated above. Presented in this study are the model configuration (physics parameters, domains used), ensembling techniques utilized, simulation results highlighting the ability of WRF to capture diurnal and intraseasonal variability (transient convective events) of moisture and dynamics of the synoptic environment (SHL, ITF, ITD), as well as examples of real-time forecasts of the moisture regime in the region of study.

Model Configuration

We selected the domains for our suite of experiments as displayed in figure 1. We use Mercator projection, a 90 km resolution for the outer domain and 30 km for the inner domain. The placement of the domain(s) conforms to the optimum configuration for important variables such as moisture advection, temperature, ITCZ location, orography. We use 5 point relaxation zone, a non-hydrostatic option and positive definite advection of moisture. The model uses National Centers for Environmental Prediction (NCEP) Final Reanalysis (FNL) as boundary conditions and daily-updating sea surface temperatures (SSTs).

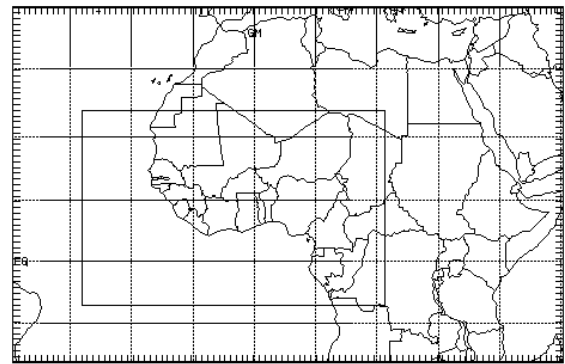


Figure 1. Inner and outer domain for WRF simulations

We ran an ensemble of simulations for the March through June period in 2006 using a variety of physics parameters in order to discern the optimal configuration of packages for our purposes. We chose 2006 because of the significant amount of station observations during the African Monsoon Disciplinary Analysis (AMMA) (Redelsperger et al., 2006) and we use the station in Niamey, Niger (13°27'N, 02°06'E) to analyze model results at a specific location. The particular physics parameters tested include cumulus parameterization, surface layer option and surface physics, boundary layer option, soil layers, microphysics schemes and radiation schemes.

Highlighted in figure 2 is the average temperature for May 2006 as portrayed by two different ensemble members where we varied only the surface physics and soil layers. Kept constant were the microphysical scheme (WSM 3), cumulus (Kain-Fritsch), surface layer (Monin-Obukhov), PBL (YSU), and radiation (CAM). Figure 2 (a) shows ensemble member 1 (E1), which has the Noah Land Surface Model (hereafter NLSM) option, and (b) ensemble member 10 (E10) with the thermal diffusion (hereafter TD) option. As is evident from the plots, the simulation using the TD option significantly underestimates the average temperatures during the month of May by about 6°C over the continent as portrayed by NCEP/NCAR Reanalysis and the European Centre for Medium-Range Weather Forecasts (ECMWF) operational simulation (not shown). As a result of this finding, we have opted to use the NLSM option for our subsequent downscaling of analyses and real-time simulations and all other options in E1 except for the microphysical scheme (WSM6). From

previous work with WRF Version 2 and a similar analysis (not shown), it became evident that the radiation schemes (Rapid Radiative Transfer Model long wave and Goddard shortwave) partially reduced the negative temperature anomalies shown on figure 2b. Further testing is still being conducted with WRF3.

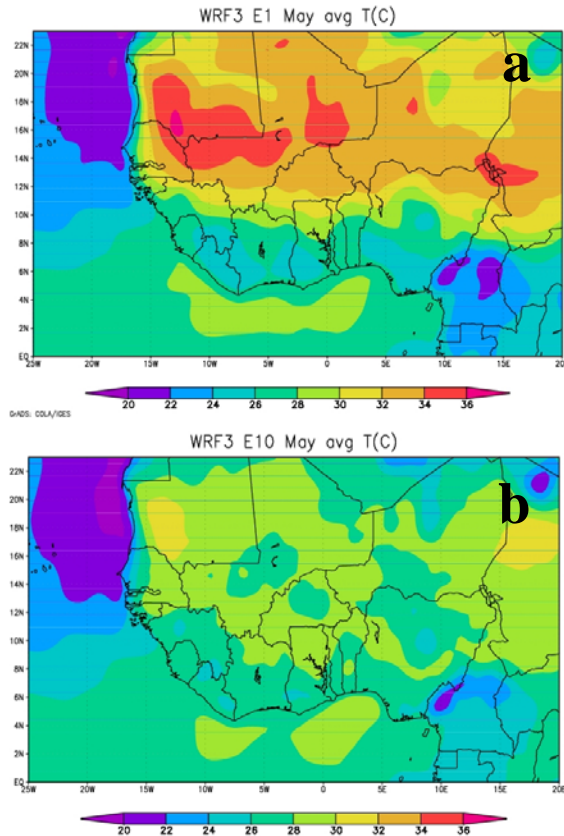


Figure 2. WRF simulations of average temperature C for May 2006 for ensemble members (described in text) e1 (a) and e10 (b).

Ensemble Prediction

In this section we discuss the ensembling techniques utilized for seasonal analysis and real-time short and medium range forecast simulations. For the seasonal analysis we limit ensemble diversity to 8 combinations of physics schemes as described in the *model configuration* section above. We have chosen relative humidity (RH, %) as a variable to analyze because of its strong relationship with meningitis outbreaks. An important figure in the literature is the 40% threshold at which the dry, dusty Harmattan air is replaced by the moister Monsoon air mass (Besancenot et al., 1997). We will use this number as our indicator for the subsequent sections. As we may discern from figure 3, there is a clear distinction between ensemble members using TD (WRF E8, E10 and E14) and NLSM (WRF E1-5) and this can be tied to the cooler conditions represented in figure 2b. This type of ensembling has yielded important variance in the simulation of RH that can be used for further refinement of physics parameterization. We note that throughout the period May 1-29 the WRF simulations nearly continuously supersede the daily RH observations gathered at the Niamey station as can be shown when the average of the NLSM ensembles (dotted) is compared to the observed (solid). We extended our use of ensemble prediction for real-time simulations of the West Africa region using Global Forecasting System (GFS) input for several forecast periods from March 4 to June 7. Instead of varying physics combinations, however,

we opted for altering initial conditions, i.e. the specific time at which the simulation was started. As an example (schematic on figure 4), for any given day you have 4 GFS forecasts issued at 00z, 06z, 12z and 18z. Out of those 4 forecasts 2 different forecasts were created. That is, we now have forecasts initialized on a 3-hourly period: 00z, 03z, 06z, etc. This technique yielded important differences in our outlooks that allow for probabilistic forecasts as can be seen in the next section.

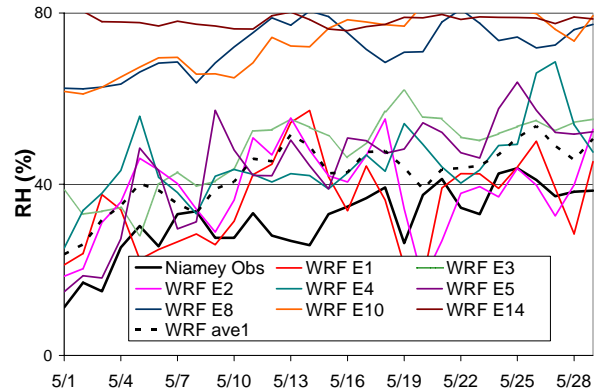


Figure 3. Relative Humidity of as given by an ensemble of WRF simulations using 8 different physics parameter combinations (color), Niamey station observation (black, solid), and LSM ensembles (black, dotted).

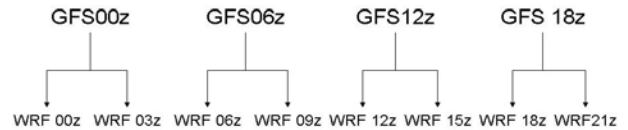


Figure 4. Schematic of real-time ensemble technique.

Intraseasonal and Diurnal variability

As we may discern from figure 3, the downscaling of FNL reanalysis captured intraseasonal variability reasonably well, with some ensemble members being able to capture specific events (extreme peaks and valleys in observations) better than others. Similarly, we also present how the model performed in terms of diurnal variability. Figure 5 shows the diurnal pattern of RH (%) for the May 23-29 period as given by the observations at Niamey (solid blue), and two ensemble members E1 (black dashed) and E2 (black dotted). These results also suggest that the model is accurately portraying diurnal variability at this specific location.

Real-time Forecasts

We performed a series of real-time ensemble simulation forecasts of relevant variables in an effort to test the capabilities of WRF for usage as a tool in meningitis mitigation efforts in West Africa. We obtained these forecasts using the initial conditions ensembling technique highlighted in the *ensemble prediction* section where we varied the initialization time. The physics parameters remained constant and follow those used in ensemble member E2, also described above. We subsequently compared our forecasts against station observations throughout the West Africa region including Niamey as in the above, as well as Kano in Nigeria (not shown), Bamako in Mali (not shown), among others. Added to station data we also compared our results against gridded NRP reanalysis and our downscaled FNL reanalysis with WRF once the boundary conditions for the forecasted period became available. We ran

two downscaling simulations: one with surface skin temperature as our varying SSTs and one with NCEP Real-time Global (RTG) SSTs at a resolution of 0.5° .

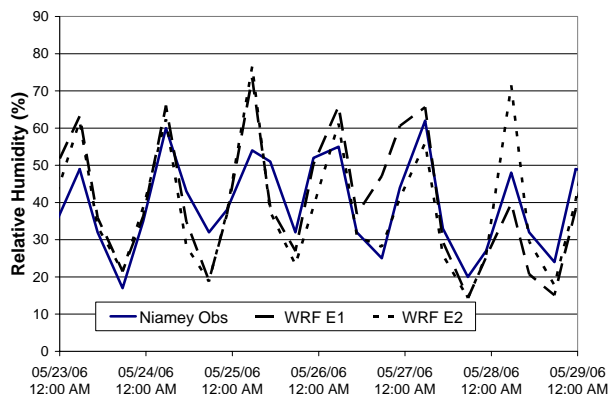


Figure 5. Diurnal variability of RH (%) as given by station data at Niamey (solid blue), and ensemble members E1 (dashed black) and E2 (dotted black).

In addition to the comparisons discussed above we also developed a website with bi-weekly forecasts generated with our ensemble analysis (climlab.meas.ncsu.edu/westafrica). These include plots showing (i) RH (%) at two meters, (ii) precipitation and 933mb winds, (iii) average surface temperatures and 10m winds and an (iv) a plot of the West Africa region showing daily anomalies of changes in RH (figure 8). For i-iii above we analyzed both daily and weekly means over the small domain in figure 1. We generated two groups of 8-member forecasts: group 1 for the first 7 days as described in the ensemble prediction section and another for the extended outlook that includes the following week (i.e. 7-15 day forecast). For the extended outlook GFS provides boundary conditions on a 12-hourly basis, so we varied our initial conditions 36 and 48 hours prior to the start of the forecast period.

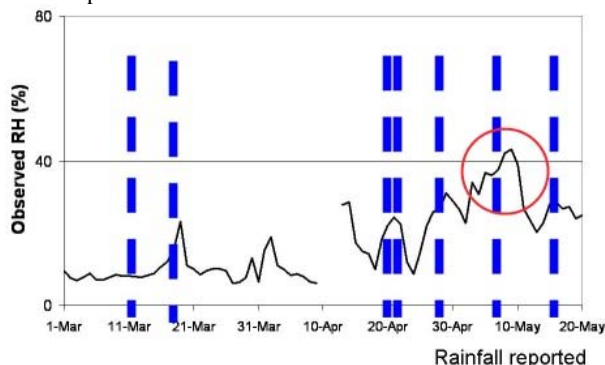


Figure 6. Relative Humidity for the March 1 – May 20 period from a station in Niamey, Niger. Blue dashed vertical lines portray precipitation events.

We found that our real-time simulations are able to capture intraseasonal variability in the moisture regime due to westward-propagating systems. In figure 6 we plotted the observed RH (%) at Niamey, Niger for the March 1 – May 20, 2009 period. In dashed blue vertical lines are days in which the station also reported precipitation. We then focused on two forecast periods adjacent to the rain event on May 7-8 and a spike in RH above the 40% threshold (circled). Figure 7a shows individual daily forecasted RH for each of the ensemble members (colors) for the May 2-7 forecast period, observed RH

(solid black), NNRP (dotted with empty squares), WRF FNL (dashed with closed circles), WRF FNL + RTG SSTs (dashed with black triangles), and the ensemble forecast average (blue circles). We note that the forecast initialized on May 1st to allow spin-up time is able to capture the temporary change in the moisture content of the atmosphere at Niamey. We can also see that there was enough spread in the results to provide a probabilistic forecast for this particular event. The second set of simulations initialized on May 7th (7b) also capture the brief period above the 40% threshold although ensembles 5-8 (initialized at 12z and 18z on May 7th) portray an elongated period ~40% until May 11th. The ensemble average (blue circles) reflects this as well. Note that NNRP and WRF reanalysis is not shown on 7b. Another potentially important factor is the difference between WRF FNL and WRF FNL + RTG SST, which although higher in resolution in terms of lower boundary input, performs worse than the former when compared with the observations. We propose that the spin-up time for higher resolution lower boundary conditions may have an effect on the final outcome of the simulation.

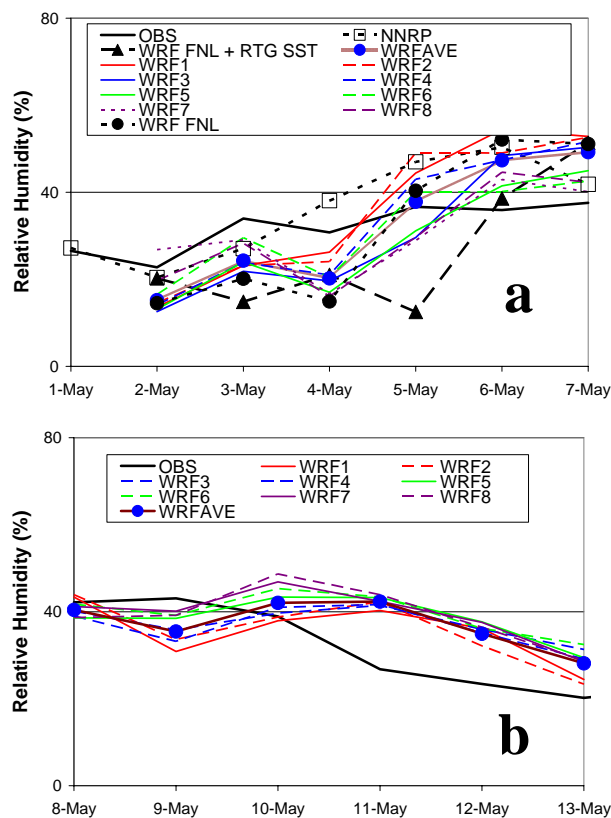


Figure 7. Time series of relative humidity (%) for the May 1-7 (a) and May 8-13 (b) where the solid black line represents station observations, colored lines are individual ensemble member forecasts, dashed triangle for WRF FNL+RTG SSTs, dotted with black circles for WRF FNL, dotted with empty squares for NNRP reanalysis and dotted with blue squares for WRF ensemble average.

The implication of transient convective systems on surface moisture is evident in our analysis and WRF allows us to trace the precipitation event on May 7-8 as well as the spike in RH to a westward-propagating disturbance. Figure 8a shows the change in RH from May 6 to May 7 and a wave-like feature of the 40% threshold (solid black curve) that extends from the 0°E to 10°E with a zenith at 20°N in extreme southern Algeria. The

anomalies show positive numbers to the west and corresponding negative numbers on the eastern side of the disturbance. This is another indication that the feature is moving westward. In figure 8b we can discern a significant amount of rainfall extending from northern Ivory Coast sloping eastward into central Niger. It's important to note that these disturbances, although temporary in nature, do increase the moisture in the air (see figure 6) bringing into a new regime (~20% to ~30%). This is a potentially important factor for meningitis mitigation efforts in this part of the world and we have showed that WRF simulations are able to capture the event.

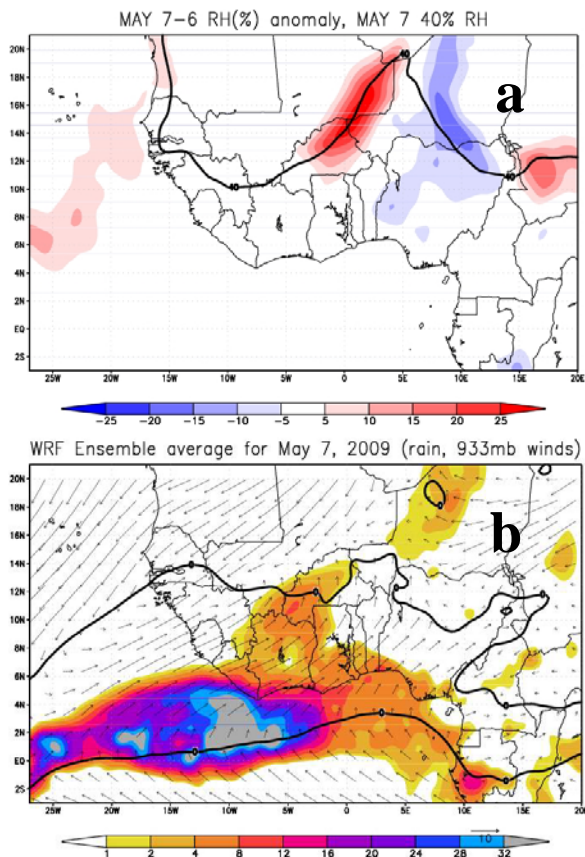


Figure 8. West Africa real-time forecasts for (a) May 7-6 day anomaly for changes in RH (%) and (b) May 7 rain totals (mm) and 933mb winds. The black line shows the position of the ITCF and is defined as u wind component equal to zero.

Concluding Remarks

Our analysis above has showed that WRF can be used to diagnose the moisture regime preceding the West African Monsoon for health efforts in the region. We diagnosed the physics parameter combinations that best suit our application and showed the significant negative temperature anomalies caused by using the TD scheme. An important feature highlighted in our real-time forecasts section is the large differences between using FNL skin temperature as lower boundary conditions and the higher resolution RTG SSTs. This pattern was also found in other forecast periods (not shown). We will devote further resources into diagnosing this disparity. Future work includes ensembling of seasonal predictions for the 2000-2009 period using both physics parameter and initial conditions techniques, data assimilation using WRF3DVAR and a new spectral nudging technique developed at North Carolina State University. High resolution seasonal downscaling of FNL reanalysis will enable us to diagnose long term regional climate

drivers, the dynamics of the WAM pre-onset and its relationship with surface moisture (diurnal process, SHL, ITF, large scale circulation patterns, etc), sensitivities (e.g. SST), and other predictive factors like transient systems (which can have an additive, step-wise process that induces a change in moisture regime at the surface at latitudinal and temporal scales). Time scales generated for useable forecasts relevant to health efforts can be from 2 to 15 days out. Further analysis will allow us to look at the different indices appropriate for meningitis mitigation (3.5,7 days of regime change), 40%, 50% + in RH.

References

- Besancenot, J.P, M. Boko and P.C. Oke, 1997: Weather conditions and cerebrospinal meningitis in Benin (Gulf of Guinea, West Africa) *Euro. J of Epidem.* **13**: 807-815
- Drobinski P, Sultan B, Janicot S. 2005. Role of the Hoggar massif in the West African monsoon onset. *Geophys. Res. Lett.* **32**: L01705
- Flamant, C., J.-P. Chaboureaud, D. J. Parker, C. M. Taylor, J.-P. Cammas, O. Bock, F. Timouk and J. Pelona, 2007: Airborne observations of the impact of a convective system on the planetary boundary layer thermodynamics and aerosol distribution in the inter-tropical discontinuity region of the West African Monsoon. *Q. J. R. Meteorol. Soc.* **133**: 1175-1189
- Flamant, C., P. Knippertz, D. J. Parker., J.-P. Chaboureaud, C. Lavaysse, A. Agusti-Panareda and L. Kergoat, 2009: The impact of a mesoscale convective system cold pool on the northward propagation of the intertropical discontinuity over West Africa. *Q. J. R. Meteorol. Soc.* **135**: 139-159
- Hagos, S.M., and K.H. Cook, 2007: Dynamics of the West African monsoon jump. *J. Climate*, **20**, 5264-5284.
- Knippertz, P., A.H. Fink, 2009: Prediction of Dry-Season Precipitation in 2 Tropical West Africa and its Relation to Forcing 3 from the Extratropics. *In press.*
- Le Barbe', L., T. Lebel, and D. Tapsoba, 2002: Rainfall variability in West Africa during the years 1950-90. *J. Climate*, **15**, 187-202.
- Lebel T, Thorncroft C, Redelsperger J-L. 2005. AMMA white book, available from <http://science.amma-international.org/science/>.
- Molesworth AM, Cuevas LE, Connor SJ, Morse AP and Thomson MC. (2003) Environmental Risk and Meningitis Epidemics in Africa. *Emerging Infectious Diseases* **9(10)**: 1287-1293.
- Parker, D.J., R. R. Burton, A. Diongue-Niang, R. J. Ellis, M. Felton, C. M. Taylor, C. D. Thorncroft, P. Bessemoulin and A. M. Tompkin, 2005: The diurnal cycle of the West African monsoon circulation. *Quart. J. Roy. Meteor. Soc.*, **131**, 2839-2860.
- Redelsperger, J.-L., C. D. Thorncroft, A. Diedhiou, T. Lebel, D. J. Parker, and J. Polcher, 2006: African Monsoon Multidisciplinary Analysis: An international research project and field campaign. *Bull. Amer. Meteor. Soc.*, **87**, 1739-1746.
- Sultan and S. Janicot, 2000: Abrupt shift of the ITCZ over West Africa and intra-seasonal variability. *Geophys. Res. Lett.*, **27**, 3353-3356.
- Sultan and S. Janicot, 2003: The West African Monsoon Dynamics. Part II: The "Preonset" and "Onset" of the Summer Monsoon. *J. Climate.*, **27**, 3353-3356.